

Experimental study on Chinese ancient timber-frame building by shaking table test

Xi-cheng Zhang*, Jian-yang Xue, Hong-tie Zhao and Yan Sui

*School of Civil Engineering, Xi'an University of Architecture and Technology, Xi'an, Shaanxi, China
State Key Laboratory of Architecture Science and Technology in West China, Xi'an, Shaanxi, China*

(Received September 11, 2009, Revised March 2, 2011, Accepted August 17, 2011)

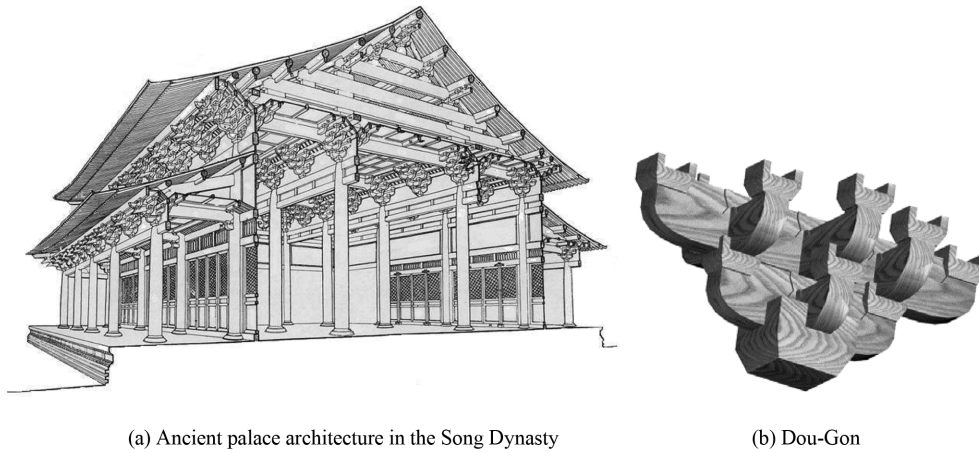
Abstract. A one-story, wooden-frame, intermediate-bay model with Dou-Gon designed according to the Building Standards of the Song Dynasty (A.D.960-1279), was tested on a unidirectional shaking table. The main objectives of this experimental study were to investigate the seismic performance of Chinese historic wooden structure under various base input intensities. El Centro wave (N-S), Taft wave and Lanzhou wave were selected as input excitations. 27 seismic geophones were instrumented to measure the real-time displacement, velocity and acceleration respectively. Dynamic characteristics, failure mode and hysteretic energy dissipation performance of the model are analyzed. Test results indicate that the nature period and damping ratio of the model increase with the increasing magnitude of earthquake excitation. The nature period of the model is within 0.5~0.6 s, the damping ratio is 3~4%. The maximum acceleration dynamic magnification factor is less than 1 and decreases as the input seismic power increases. The frictional slippage of Dou-Gon layers (corbel brackets) between beams and plates dissipates a certain amount of seismic energy, and so does the slippage between posts and plinths. The mortise-tenon joint of the timber frame dissipates most of the seismic energy. Therefore, it plays a significant part in shock absorption and isolation.

Keywords: Chinese palace buildings; timber structure; seismic performance; shaking table test

1. Introduction

Chinese ancient architecture is a special system that has a unique style. It differs greatly from western traditional buildings in many aspects: material, structural system, space layout, and cultural values. Buildings in many countries such as South Korea, Japan are deeply influenced by China's architectural style. Among the majority of ancient buildings, the timber-frame structure is the most common form, constituting around 50% of all the buildings. In particular, such buildings as palaces (Fig. 1(a)), shrines and temples have a structural member named Dou-Gon (see Fig. 1(b)) on them. Dou-Gon is a bracket system which consists of Dou and Gon. Gon is a bow-shaped arm which supports a block of wood, called Dou on both ends. It is usually inserted between the top of a column (or a lintel) and a cross beam (Fig. 1(a)) as a connection. Structural members such as beams, columns and purlins are connected by mortise-tenon joints (Fig. 2) which have various types, shapes and dimensions. There are no nails or bracing used in the timber frame. A post is

*Corresponding author, Ph.D., E-mail: xicheng-zhang@163.com



(a) Ancient palace architecture in the Song Dynasty

(b) Dou-Gon

Fig. 1 Typical timber ancient architecture with Dou-Gon

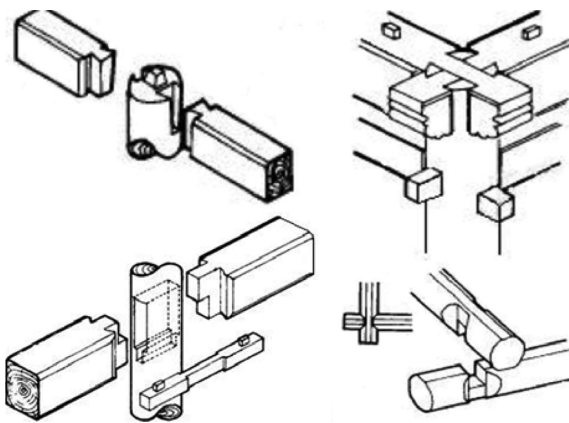


Fig. 2 Mortise-tenon connection

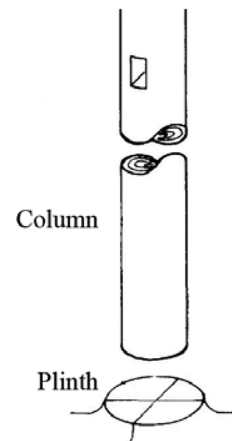


Fig. 3 Column simply supported on plinth

simply laid on top of a cornerstone (plinth), and the plinth is anchored in the foundation of a building, as shown in Fig. 3.

The earliest Chinese timber architecture that has ever been found is 5,000 years old, and the first book on the fabrication and construction of timber structures (Li 1100) was published in the Song Dynasty (A.D.960-1279). Liang (1984) and his colleagues took the first step to study on the architectural and structural styles of ancient timber structures. Their work laid the foundation of the subsequent studies for all the ancient architecture researchers. In order to provide theoretical support on the maintenance of these precious heritages, more and more studies started to focus on the structural behavior of ancient timber structures. As the joint of this type of structure is very special, much attention had been paid on the connections that made timber structures different. Brungraber (1985) made test on joints of a few frames. He performed 2D finite-element analyses on joint details and proposed a three-spring joint model for frame analysis. The Subcommittee on Wood Research of the ASCE Committee on Wood (1986) pointed out that joints often are the weakest link in wood structures. A joint may transfer compression, tension, and shear loads from one structural

element to another. Due to the variety of joint-type configurations, there are limited research results on the stiffness of the ancient timber joints. King *et al.* (1996) studied the static linear and nonlinear properties of plug-slot type connections by both experimental and numerical modeling methods, and found out that the stiffness of the semi-rigid connection was seriously decreased by a component's surface deterioration. Dou-Gon not only takes on an elegant appearance, but also played a significant part in structural behavior. Hayashi *et al.* (1998) studied on the restoring properties of a wooden frame with masu-gumi (Dou-Gon layers) and plug-slot connections (tenon joints) in an ancient Japanese timber structure. They pointed out that embedding of the edges of the masu (Dou-Gon layers) and the slip between each member induce most of the structural deformations, and the structural performance varies with the level of vertical load. Zhao *et al.* (1999) studied the dynamic characteristics of Dou-Gon experimentally. The test results indicated that the nature period and damping ratio varied with the axial loads. Seo *et al.* (1999) carried out experimental research on the static and cyclic behavior of Korean ancient wooden frames with tenon joints under lateral load. Although the structures in their work have similar characteristics with Chinese ancient timber architectures, there are no Dou-gon (corbel brackets) used in their structures. The dynamic characteristics of the existent ancient architecture had also been measured. Based on constant vibrator-forced vibration, micro vibration, and manpower-forced vibration tests, Yanagisawa *et al.* (1998) conducted cyclic load and vibration tests on a true Japanese temple and observed the natural frequency and damping factor of the first mode. The natural frequencies were found to be within 1~2 Hz and the damping factor to be within 1~3%. Maekawa and Kawai (1998) conducted micro tremor tests on six one-floor traditional Japanese timber houses and found that the damping factor was 1~2% and the average primary natural frequency was 3 Hz. Uchida *et al.* (1998) conducted more measurements on one- and two-story traditional timber buildings and multistory pagodas in Japan. The natural frequencies were found to be within 1.45~2.15 Hz for one- or two-story buildings and within 0.85~0.9 Hz for multistory pagodas. They developed a horizontal lumped mass system model applicable to one- or two-story buildings and a vertical lumped mass system model applicable to pagodas. Che *et al.* (2006) studied on the dynamic structural characteristics of an ancient Chinese architecture-Yingxian Wooden Pagoda. Based on micro tremor measurements, they achieved predominant frequency peak values of 2.5~3.5 Hz and the first three natural frequencies which were 0.6 Hz, 1.66 Hz and 2.93 Hz respectively. The results showed that the relative horizontal displacement under earthquake would concentrate on the second floor. To enhance the understanding of dynamic and seismic properties of ancient timber structures and to provide information and suggestions for their protection and maintenance, Fang *et al.* (2001) conducted full-scale on-site tests and model tests on the front tower over the North Gate of the Xi'an City Wall. The first four natural frequencies of the structure were found to be 1.10, 1.70, 2.73 and 3.10 Hz, respectively. D'Ayala and Tsai (2008) performed a preliminary FE linear analysis on Taiwan's traditional temple structure showing that the stiffness of the timber joints is important in changing the magnitude of the overall displacement of the building. Ten laboratory tests were conducted on the set joints showed that their rotational stiffness depends on the vertical load applied to the joint while the translational stiffness is not affected by the vertical load applied. Meng *et al.* (2009) carried out dynamic response tests on timber structure of Xi'an Bell Tower to inspect to the influence of micro-vibration excited by vehicles. They found that the vibration levels of upper floor are enlarged obviously than the column foundation. Tsou *et al.* (2000) investigated the wind resistance of a traditional Chinese temple using numerical and experimental methods. The numerical simulation shows that the absolute values of negative pressures on the roof reach the maximum along the drooping ridges, and that the owl tails

at the top of roof can share the negative pressure on the roof. After Wenchuan earthquake, many ancient buildings were damaged or collapsed. Zhou and Yan (2009) investigated Da-Xiong Palace which is 189 km far away from the epicenter and found columns inclined. They studied responses of displacement and stress of the structure and the results showed that the main reason for incline of columns of the structure was that tenon pulled out from mortise of some tenon-mortise joints between tie beams and columns.

Far East Asian ancient timber structure derives from buildings in China's Tang Dynasty. It has an architectural style of Tang period and has made developments in its own way. Compared with Tang-style timber structures, there is a decrease on all aspects of construction scope and configuration in Song-style buildings. So, there are major differences in arrangement and dimensions of structural members between Far East and Song-style buildings. Accordingly, the data obtained from current researches of Far East timber structures can not be directly taken. But there is something still in common between these two different styles, such as the use of mortise-tenon joint and Dou-Gon sets which make timber building a long-period and antiseismic structure. There are many Song-style palace buildings which are old and on the edge of destruction in China. But in fact, the experimental study on the structural behavior of this kind of structure has not been conducted yet. Only a few post earthquake surveys can be used for reference (Chinese Academy of Sciences 1956).

This paper describes a research program that presents results from shaking table tests of a one-story wood frame building with the effort to quantify the seismic performance of Chinese ancient timber buildings with Dou-Gon layers.

2. Shaking table test

2.1 Specimen and instrumentation

Fig. 4 shows the specimen tested in this study. Taking into account the limitation of shaking table's dimension, an intermediate bay model with four posts is extracted from the original building. Then it was fabricated strictly according to the Building Standards of the Song Dynasty (A.D.960-

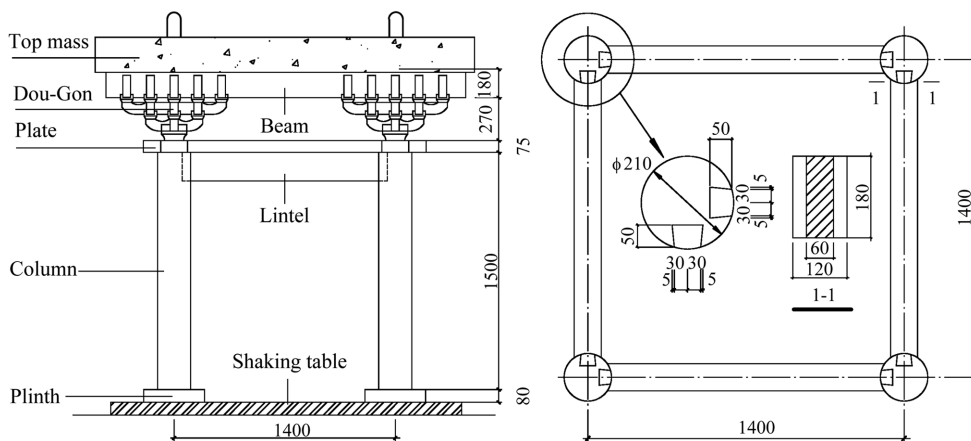


Fig. 4 Test specimen

1279). The column diameter is 210 mm. The material of the specimen is Korean pine imported from Russia. Bluestone is selected as the material of the plinth which is fixed on the shaking table with four anchor bolts. The surface of stone plate is roughly polished. The wooden frame is placed directly on the top of the four stone plinths. The joint of the frame is the swallowtail-tenon and mortise connection. On top of the lintel, there is a plate (1600 mm × 180 mm × 75 mm) connected with the two posts on the top. The Dou-Gon layers called column sets are placed on the surface of the plates, right on top of the posts. As there is no intermediate Dou-Gon set on the plate which is on top of the lintel, the roof's weight is equally shared on the four upper beams of the frame and then transmitted to four posts below column sets. The model is an intermediate bay, i.e., a central part of the whole building. So the roof can not be made properly by the whole structure's construction. The load from the roof was simplified as the weight of a concrete block. According to the real loading area of the four-post model, the total weight of the roof can be calculated. The equivalent mass of the concrete plate is equal to 3600 kg.

In considering the relationship between existing length units and Song foot and the limiting dimension of the shaking table, the model was designed to 1:3.52 scale, i.e., a length ratio of 0.284. Other scaling parameters are shown in Table 1.

Fig. 5 demonstrates the arrangement of test instruments. 15 varactor-based accelerometers and 12 electromagnetic sensors were installed to record the shake table, column, and beam absolute acceleration, velocity and displacement time histories at several locations in the structure. At both column and lintel ends near the joint, strain gauges were placed to measure the strain changes in order to calculate the inner force of the swallow-tail tenon joint. As well, three video cameras were used to record each seismic test.

Table 1 Scaling parameters of the model

Basic parameters	Surface load ratio	Length ratio	Stress ratio	Acceleration ratio	Time ratio	Velocity ratio	Elasticity modulus ratio
Ratios	1	1/3.52	1	1	$1/\sqrt{3.52}$	$1/\sqrt{3.52}$	1



Fig. 5 Test set-up and arrangement of instruments

2.2 Testing procedure

The shaking table tests were performed on the 2 m × 2.2 m unidirectional earthquake simulation facility of the State Key Laboratory of Architecture Science and Technology in West China at Xi'an Univ. of Architecture & Technology, China. El Centro (N-S), Taft wave and Lanzhou wave were selected as the input ground motions. The ground motions were scaled using a time scale factor equal to 0.53 considering the similitude requirements of the specimen. These three waves were used before motivating the input peak acceleration to 300 gal. The input ground motion is 50 gal, 75 gal, 150 gal, 200 gal and 300 gal respectively. For the following test sequences, only El Centro wave was inputted. Each input level is 400 gal, 500 gal, 600 gal, 700 gal, 800 gal, and 1000 gal. There were modal tests to estimate the fundamental frequencies and mode shapes of the model between each level of input excitation. Finally, the collapse test was conducted under sine wave excitations with frequency of 2 Hz, 1 Hz and 0.5 Hz respectively.

3. Experimental results

3.1 Observations

When the model was subjected to minor earthquakes, there was no noticeable shaking and no slippage between posts and plinths. In the case of moderate earthquakes, the model responded with increasing amplitude. A “creak” sound of friction could be heard. When the earthquake excitation reached 300 gal, the column roots began to slip slightly. The Dou-Gon layers began to make a small slip as the acceleration of El Centro wave reached 400 gal. With the gradual increase of seismic excitations, the response of the model was also growing. The joint rotated due to deformation of tenon and mortise, and the tenon was pulled out a bit, as shown in Fig. 6(a). When the table acceleration was motivated to 900 gal, the residual displacement of the column roots reached about 50 mm, as shown in Fig. 6(b). Though the lateral deformation was already quite large, the frame remained as a whole retaining its strength and stability. In order to ensure the safety of instrumentations, all the sensors were removed and the top mass are suspended by the crane during the collapse test. With the continuing increase of sine wave excitation (0.5 Hz), the model reacted strongly, the pull-out of the tenon increased. Finally the mortise damaged, and the tenon was



(a) Pullout of the tenon

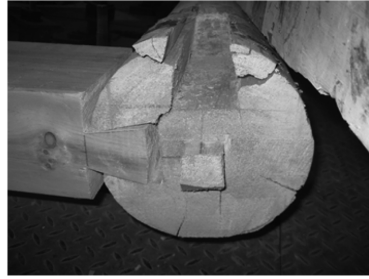


(b) Slippage of plinth

Fig. 6 Test phenomena



(a) The tenon broke



(b) The mortise split



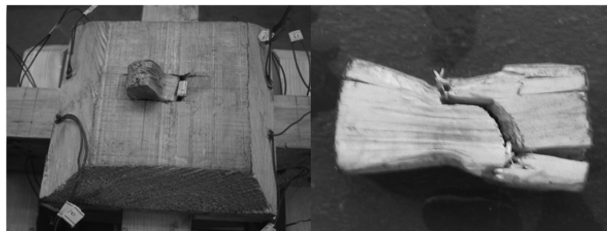
(c) The collapse of the specimen



(d) Rotation of Dou-Gon



(e) Dou-Gon after collapse



(f) Shear failure of tenon at the bottom Dou

Fig. 7 Failure pattern of the specimen

completely pulled out, resulting in the collapse of the model, as shown in Fig. 7(a), (b), (c). In the whole process of each seismic excitation, Dou-Gon played the role as a planar hinge and rotated along the vibration direction of shaking table, as shown in Fig. 7(d). As the collapse occurred, the Dou-Gon joint set fell on the ground and scattered. After every single member (Dou and Gon) was reassembled, the whole set remained intact, as shown in Fig. 7(e). But there was material failure occurred in some of small tenons at the bottom of Dou, as can be seen in Fig. 7(f). It corresponds to China's post earthquake surveys (Chinese Academy of Sciences 1956).

3.2 Displacement and acceleration responses

Table 2 compiles the maximum displacements and accelerations in different locations of the model. It indicates that displacement and acceleration responses of the model increase along with the increasing input excitations. The column head's displacement is the biggest among each layer's displacement peaks. The maximum displacements of the top beam and the lower column root under different input levels are relatively smaller than that of the column head. Among different layers' acceleration peaks, the value of column root is the biggest. The upper layers' accelerations become smaller than the column. It shows that the input acceleration decreases as a result of the mortise-tenon-joint frame. This mortise-tenon joint has a capability of energy dissipation and shock absorption. Table 2 also shows that the peak acceleration of column is less than that of the input ground motion. So there must be a relative slippage between the column root and the plinth.

The displacement and acceleration responses under various seismic excitation of El Centro wave are shown in Fig. 8.

As can be seen from Fig. 8, in the case of minor earthquakes, the peak point in time-displacement curve of the upper beam and the table occurs simultaneously. The time-acceleration history curve of the upper beam coincides largely with that of the table. At this period, the structure's effect of vibration isolation and absorption is not obvious. When subjected to moderate earthquakes, there is a time lag for the peak value in the time-displacement curve of the beam and table. The acceleration value of the top beam is less than that of the bottom table. The effect of vibration isolation and absorption is significant. When subjected to major earthquakes, time lag of the peak displacement

Table 2 Peak values of displacements and accelerations

Input ground motion	Table acceleration (gal)	Column root displacement (mm)	Column root acceleration (gal)	Column head displacement (mm)	Column head acceleration (gal)	Top displacement (mm)	Top acceleration (gal)
El Centro	51	4.261	46	6.255	34	6.352	37
	141	10.118	121	15.868	59	16.212	64
	291	22.874	259	36.475	107	30.324	92
	551	45.914	499	67.372	132	43.526	111
	901	120.613	861	221.502	199	110.636	118
Taft	50	4.344	42	6.769	33	6.573	38
	144	11.217	136	21.203	69	17.454	73
	283	21.747	246	39.616	82	29.358	86
Lanzhou	48	5.444	45	7.447	26	7.043	27
	126	15.231	24	24.966	68	23.999	62
	253	45.117	235	72.299	114	47.005	94

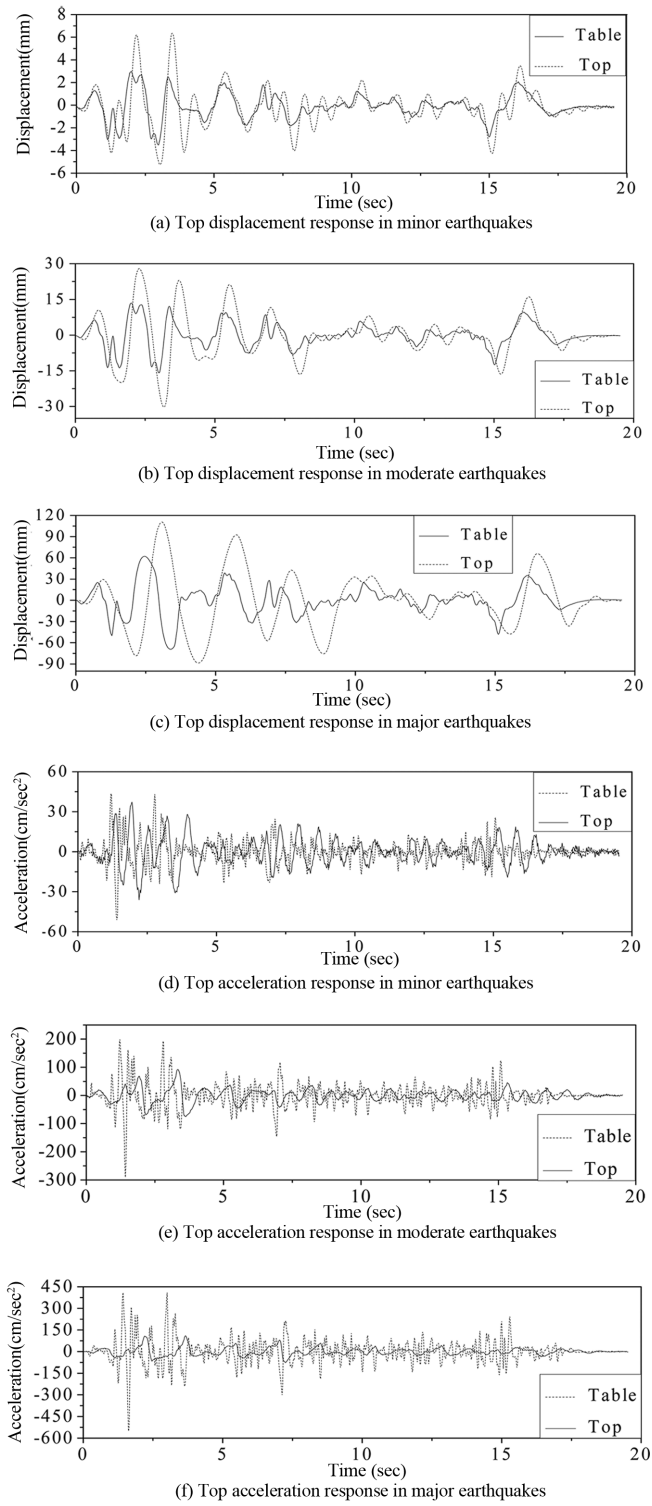


Fig. 8 Displacement and acceleration responses

increases. The difference between the acceleration of the table and beam also increases significantly. It is indicated that the seismic capacity of the timber structure enhances greatly.

3.3 Dynamic magnification factors

According to construction forms of the ancient timber building, we can divide the structure into four parts: the roof layer above, the Dou-Gon layer under beams, the post-and-lintel frame layer, and the plinth layer below. All four parts play an important part in earthquake isolation and dissipation. In order to quantify their contributions, the dynamic magnification factors are introduced. The maximum acceleration dynamic magnification factors obtained from the testing results are shown in Table 3. β_1 is the ratio of the maximum absolute acceleration of the column root to the maximum input ground acceleration. It accounts for the effect of earthquake isolation through slippage between post and plinth. β_2 is the ratio of the maximum absolute acceleration of the column capital to that of the column root. It reflects the shock-absorption capability of the mortise-tenon joint. β_3 is the ratio of the maximum absolute acceleration of top beam to that of column capital. It provides a quantitative index of the shock-absorption capability of the Dou-Gon layers. β_4 is the ratio of the ratio of the maximum absolute acceleration of top beam to the maximum input ground acceleration. It reflects the effect of vibration isolation and absorption of the whole structure.

Table 3 indicates that the plinth and mortise-tenon joint began to play a role in vibration isolation and shock absorption respectively when subjected to minor earthquakes. With the increase in input seismic excitation, β_1 changed a little while β_2 reduced significantly. It shows that the frictional slippage between plinth and column made little change in earthquake isolation, but the mortise-tenon joint played a growing role in seismic energy dissipating and shock absorption. β_3 is greater than 1 subject to minor earthquake, but less than 1 when in higher acceleration. It mainly depends on the configuration of Dou-Gon. According to the test phenomena, Dou-Gon set makes translational motion together with the upper beam in minor acceleration, but there is no deformation occurred in Dou-Gon itself. In major seismic excitation, Dou-Gon set not only makes horizontal displacement along with the upper beam but also rotates in the direction of vibration. Therefore, there are compression and friction occurred between Dou and Gon. Finally, plastic deformation is observed in the small tenon which connects Dou and Gon (Fig. 7(f)). It's a shear failure. It's the deformation

Table 3 Dynamic magnification factor

Input ground motion	Table acceleration (gal)	β_1	β_2	β_3	β_4
El Centro	51	0.892	0.742	1.101	0.728
	141	0.852	0.493	1.077	0.452
	291	0.892	0.414	0.857	0.317
	551	0.906	0.264	0.834	0.2
	901	0.955	0.231	0.598	0.132
Taft	50	0.851	0.779	1.142	0.757
	144	0.944	0.508	1.063	0.509
	283	0.868	0.335	1.049	0.305
Lanzhou	48	0.948	0.569	1.071	0.577
	126	0.984	0.553	0.903	0.492
	253	0.927	0.485	0.828	0.373

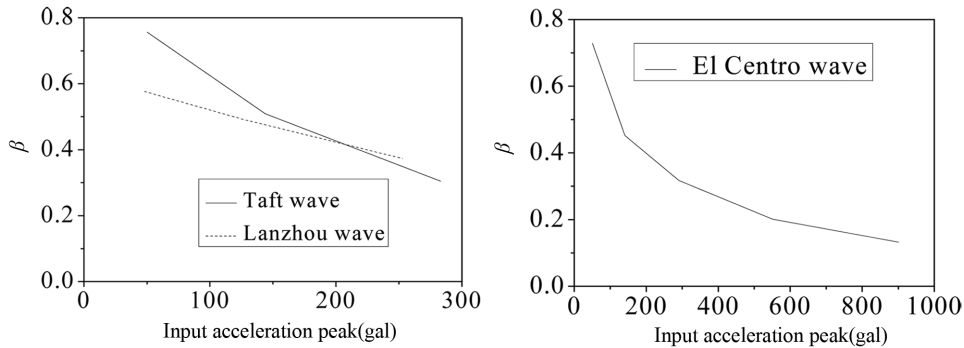


Fig. 9 Dynamic magnification factor

dissipates the seismic energy. Hence, the Dou-Gon layers' effect of earthquake isolation was not obvious in the case of minor earthquakes. It began to work in moderate earthquakes and increased as the input seismic excitation increased. Fig. 9 shows changes of the maximum acceleration dynamic magnification factor β_4 under different levels of earthquakes.

As can be seen from Fig. 9, the maximum acceleration dynamic magnification factors of the whole structure decreased as input ground motion increased. When subjected to minor earthquakes, β_4 is about 0.7. And in the case of moderate and major earthquakes, β_4 reduces to 0.3 and 0.1 or so respectively. The results indicate that the structure has a good capacity in energy dissipation.

3.4 Nature periods and damping ratios

The nature periods obtained from model tests are shown in Table 4. From the table, it can be seen that the nature period T of the timber-frame model increased as the seismic excitation increased, which shows that the stiffness of the structure decreased due to cumulative damage.

According to free vibration curves recorded by instruments, the damping ratio ξ of the structure can be calculated based on the following equation

$$\xi = \frac{1}{2\pi} \ln \frac{a_i}{a_{i+1}} \quad (1)$$

Where ξ refers to damping ratio of the structure, a_i and a_{i+n} represent displacement peaks in the

Table 4 Natural period after different earthquake levels

	Before testing	After minor earthquakes	After moderate earthquakes	After major earthquakes
Period T (sec)	0.48	0.54	0.6	0.63

Table 5 Damping ratios of the specimen

	Before testing	After minor earthquakes	After moderate earthquakes	After major earthquakes
ξ	0.029	0.033	0.037	0.042

free vibration curves. The damping ratios of the model are shown in Table 5.

As can be seen by Table 5, the damping ratio of the model increases with the increased intensity of seismic excitation, and it is generally between 3~4%. This shows that the wooden structure has a good capability in damping energy dissipation.

3.5 Internal force analysis

During the tests, strain gauges placed at the ends of column and lintel near the joint recorded real-time strain data, on which the moment of the joint can be calculated. The moment-angle curve of the joint is shown in Fig. 10.

When subjected to minor earthquakes, the moment M of the joint was small, and the rotation angle ν was almost 0. The area of the envelope hoop is very small, and the curve approximates to be linear. The joint is in the elastic stage. In the moderate earthquakes, the area of the envelope hoop increased. The effect of energy dissipation of the mortise-tenon was obvious. The joint came into elastic-plastic phase. In the case of major earthquakes, the area increased quickly, and the capability of earthquake energy dissipation was fully performed.

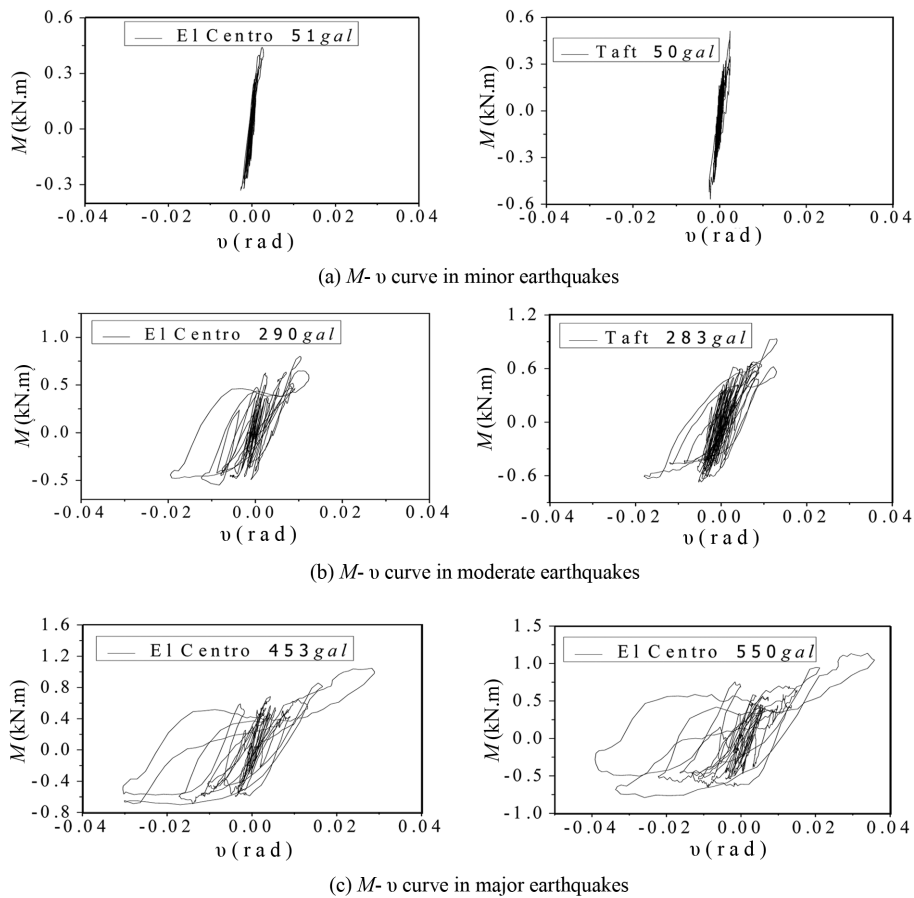


Fig. 10 M - ν hysteresis curves

3.6 Energy dissipation performance

Shear forces of the specimen in different structural layers can be calculated by the following equation

$$V_k(t_i) = \sum_k^n m_k x_k''(t_i) \tag{2}$$

In which $V_k(t_i)$ represents the shear force of the number k layer at time t_i , $x_k''(t_i)$ represents the absolute acceleration of the layer k at time t_i , m_k represents the mass of the number k layer. The shear force-displacement curves under different levels of earthquakes are shown in Fig. 11.

The energy dissipated in different layers of the specimen at different levels of earthquakes is given by

$$E_{hk} = \sum_{i=1}^m \frac{1}{2} [V_k(t_i) + V_k(t_{i-1})] [\Delta x_k(t_i) - \Delta x_k(t_{i-1})] \tag{3}$$

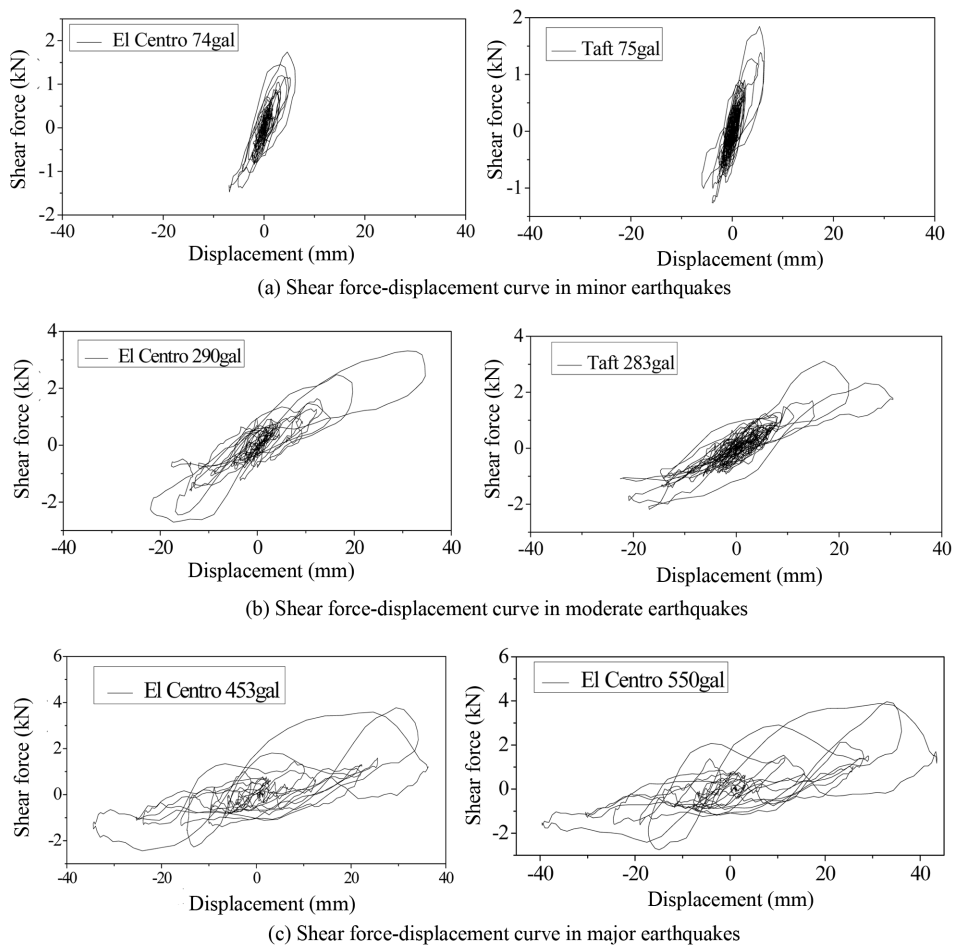


Fig. 11 Shear force-displacement hysteresis loops

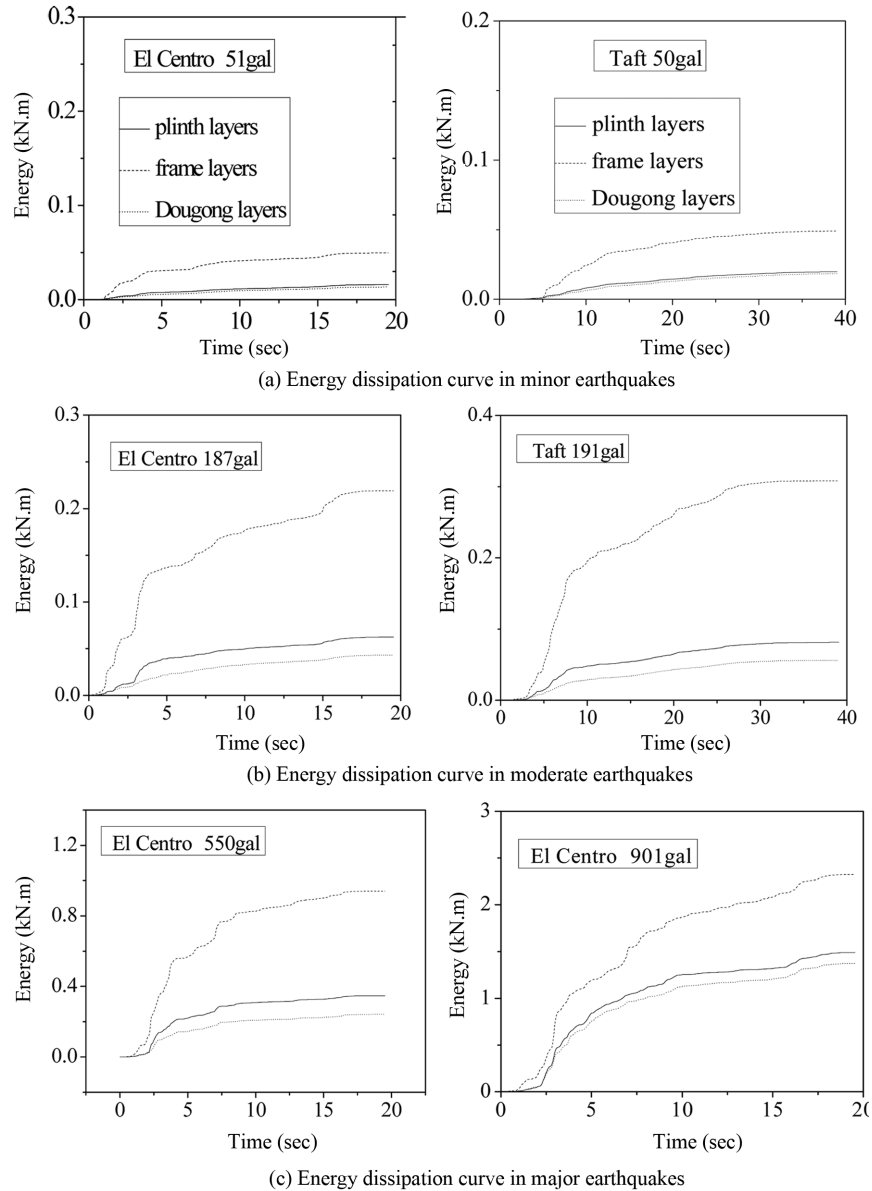


Fig. 12 Energy dissipation curves under various levels of earthquake excitations

In which E_{hk} represents hysteretic energy dissipated by layer k , and m is the total number of sampling points during loading time. Δx_k represents drift of layer k . Fig. 12 shows cumulative seismic energy dissipations of different layers under different earthquake magnitudes.

As can be seen from Fig. 12, the model dissipates seismic energy mainly by compressive deformation of the mortise-tenon joint. The effect of energy dissipation due to slippage of both plinth and Dou-Gon layer is similar. But the energy dissipated by plinth slippage is slightly higher. The larger the seismic excitation is, the bigger the effect will be.

3.7 Analysis on sliding isolation of column root and Dou-Gon set

The acceleration relation curve of column root and ground motion is given in Fig. 13 when subjected to El Centro wave.

As can be seen in this figure, the acceleration of ground motion shows a linear correlation with that of column root. By means of linear fitting treatment, a straight line is obtained. The line's slope K can be used to represent the effect of sliding isolation caused by slippage between column root and plinth. K is an average magnification factor. Table 6 lists the values of K under different input levels of El Centro wave.

All the K values listed in the Table 6 are less than 1, and the mean value is 0.89. It shows that the average magnification factor K basically remains a constant as the input excitation increases, i.e., K values are not affected by the magnitude of seismic excitations. Colum root plays a significant part in seismic isolation by its slippage on the plinth. And the sliding isolation performance is steady.

Accordingly, the acceleration relation curve of column head and the top roof can also be fitted into straight line. The slope of fitting line reveals the seismic isolation capability of Dou-Gon. K values under different input levels of El Centro wave are shown in Fig. 8.

Table 7 shows that the average magnification factor K of Dou-Gon declines as the input seismic excitation increases, which is different from that of column root. The magnitude of seismic excitation is a key factor to determine the isolation capability of Dou-Gon. The larger the input magnitude becomes, the better the isolation effect is. The mechanism of seismic isolation and

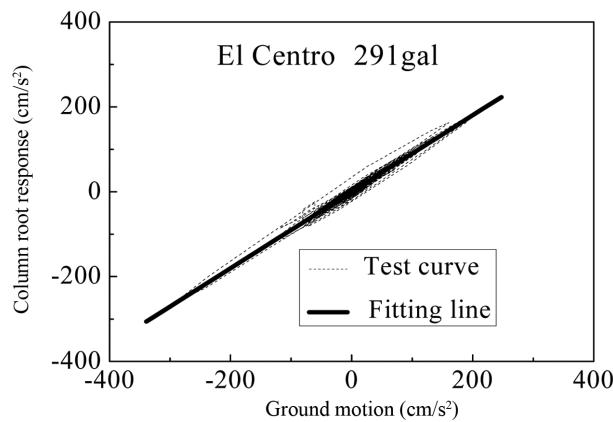


Fig. 13 Acceleration relation curve of column root and ground motion

Table 6 K values under different input levels of El Centro wave

Input level (gal)	74	142	291	551	779	901
K	0.87	0.89	0.9	0.88	0.87	0.9

Table 7 K values under different input excitations

Input level (gal)	74	142	291	551	779	901
K	1.05	1.04	0.91	0.76	0.61	0.59

absorption between column root and Dou-Gon layer is different. There is only friction slippage between column root and plinth. Apart from friction slippage between Dou and the lower plate (or lintel), Dou-Gon's horizontal deformation also dissipates a certain amount of seismic energy. Dou-Gon layer has a dual characteristic of sliding isolation and damping dissipation. As the input excitation increases, the capability of damping dissipation becomes greater. That accounts for the declining K factors along with the increasing input excitations.

4. Analysis on seismic behavior of the prototype

According to the similarity law between the specimen and prototype, the seismic behavior of prototype structure can be achieved:

1. The natural period and damping ratio of the prototype is 0.9 s and 0.029 separately. Both the two factors increased as the input ground motion enhanced, which can account for the excellent seismic behavior of the timber-frame structure. Among all the factors that make Chinese ancient timber building a long-period structure, the semi-rigid mortise-tenon joint of the beam-to-column connection is certainly a major contributor. But test shows the model finally turns into a mechanical system as a result of the failure of beam-to-column joint. So it can be concluded the mortise-tenon joint is a weak part of the prototype structure.
2. When subjected to input excitations less than 300 gal, the members of the structure are still in the elastic stage. As the excitation increases, the displacement at the top of the structure becomes larger and larger. Plastic deformation occurs in the mortise-tenon joint, and the tenon is pulled out a little from the mortise. When excitation reaches to 900 gal, the lateral displacement of the building is quite large, and the tenon is pulled out larger and larger. But the structure does not collapse.

5. Conclusions

A model representing a Chinese ancient timber-frame building was constructed in 1:3.52 scale. Shaking table tests were conducted and the model was subjected to earthquake actions. Based on the experimental results obtained, the following conclusions can be drawn:

1. The natural period and damping ratio of the specimen increased with the increasing seismic excitation. The natural period T changed in the range of 0.5-0.6 s, while the damping ratio varied from 3% to 4%. It indicates that the ancient timber-frame building is a long-period and low-frequency structure. This type of structure has a good damping energy dissipation capacity.
2. The maximum acceleration dynamic magnification factors were less than 1 and decreased along with the increasing input seismic power. It shows the structure's high capability in earthquake energy absorption and dissipation.
3. Column root and plinth dissipated seismic energy by means of frictional slippage. Dou-Gon layer has a dual characteristic of sliding isolation and damping dissipation. The mortise-tenon joint performed the strongest capability in energy dissipation, and played an important part in shock absorption and energy dissipation.

Acknowledgements

The work presented herein was carried out at Xi'an Univ. of Architecture and Technology in China, and was funded by Chinese National Natural Science Foundation under granted No. 59878043. The project was also funded by Shaanxi province as a key laboratory construction project under granted No. 05JS17. The financial support provided by these funding agencies is gratefully acknowledged.

References

- Brungraber, R.L. (1985), "Traditional timber joinery: A modern analysis", PhD dissertation, Stanford Univ. Palo Alto, Calif.
- Che, A.L., He, Y., Ge, X.R., Iwatate, T. and Oda, Y. (2006), "Study on the dynamic structural characteristics of an ancient timber -Yingxian Wooden Pagoda", *Soil Rock Behav. Model.*, 390-398.
- Chinese Academy of Sciences (1956), *Chinese Chronology of Seismic Data*, Science Press, Peking, China. (in Chinese)
- D'Ayala, D.F. and Tsai, P.H. (2008), "Seismic vulnerability of historic Dieh-Dou timber structures in Taiwan Engineering Structures", *Eng. Struct.*, **30**, 2101-2113.
- Fang, D.P., Iwasaki, S., Yu, M.H., Shen, Q.P., Miyamoto, Y. and Hikosaka, H. (2001), "Ancient Chinese timber architecture I: Experimental study", *J. Struct. Eng.-ASCE*, **127**(11), 1348-1357.
- Fang, D.P., Iwasaki, S., Yu, M.H., Shen, Q.P., Miyamoto, Y. and Hikosaka, H. (2001), "Ancient Chinese timber architecture II: Dynamic characteristics", *J. Struct. Eng.-ASCE*, **127**(11), 1358-1364.
- Hayashi, T. et al. (1998), "Restoring properties of Japanese traditional wooden frame", *Proc., World Conf. on Timber Engrg.*, Presses Polytechniques et Universitaires Romandes, Montreux, Switzerland.
- King, W.S., Yen, J.Y. and Yen, Y.N. (1996), "Joint characteristics of traditional Chinese wooden frames", *Eng. Struct.*, **18**(8), 635-644.
- Li, J. (1100), *Building Standards of the Song Dynasty*, Royal Press, Kaifeng, China. (in ancient Chinese)
- Liang, S.C. (1984), *A Pictorial History of Chinese Architecture*, Ed. W. Fairbank, MTT Press, Boston.
- Maekawa, H. and Kawai, N. (1998), "Microtremor measurement on Japanese traditional wooden houses which are important cultural properties", *Proc., World Conf. on Timber Engrg.*, Presses Polytechniques et Universitaires Romandes, Montreux, Switzerland.
- Meng, Z.B., Chang Y.Z., Song L. and Yuan J. (2008), "The effects of micro-vibration excited by traffic vehicles on Xi'an Bell Tower", *ICTE2009*, 39-42.
- Seo, J.M., Choi, I.K. and Lee, J.R. (1999), "Static and cyclic behavior of wooden frames with tenon joints under lateral load", *J. Struct. Eng.-ASCE*, **125**(3), 344-349.
- Subcommittee on Wood Research of ASCE Committee on Wood (1986), "Structural wood research needs", *J. Struct. Eng.-ASCE*, **112**(9), 2155-2165.
- Tsou, J.Y. and Zhu, Y.M. (2000), "Wind resistance of traditional Chinese temple", *Comput. Civil Build. Eng.*, 951-958.
- Uchida, A. et al. (1998), "Dynamic characteristics in Japanese traditional timber buildings", *Proc., World Conf. on Timber Engrg.*, Presses Polytechniques et Universitaires Romandes, Montreux, Switzerland.
- Yanagisawa, K. et al. (1998), "Study on earthquake-protection of traditional Buddhist temples", *Proc., World Conf. on Timber Engrg.*, Presses Polytechniques et Universitaires Romandes, Montreux, Switzerland.
- Zhoa, J.H., Yu, M.H., Yang, S.Y. and Sun, J.Y. (1999), "An experimental study for the dynamic characteristics of "Dougong"-one of the wooden structure parts in ancient architecture of China", *J. Exper. Mech.*, **14**(1), 106-112. (in Chinese)
- Zhou, Q. and Yan, W. (2009), "Damage analysis on a Chinese ancient building by wenchuan earthquake", *2009 International Joint Conference on Computational Sciences and Optimization*, 258-261.